Volumetric parcellation methodology of the human hypothalamus in neuroimaging: Normative data and sex differences

Nikos Makris [a,b,c,d], Dick F. Swaab [e], Andre van der Kouwe [d,f], Brandon Abbs [d,g,h,i,j], Denise Boriel [c,d], Robert J. Handa [k], Stuart Tobet [l], Jill M. Goldstein [a,d,g,h,i,j,*]

[a] Department of Psychiatry, Massachusetts General Hospital (MGH), 149 13th Street, Charlestown, MA 02129, USA
[b] Department Neurology, Massachusetts General Hospital (MGH), 149 13th Street, Charlestown, MA 02129, USA
[c] MGH Center for Morphometric Analysis, 149 13th Street, Charlestown, MA 02129, USA
[d] MGH & MIT Athinoula Martinos Biomedical Imaging Center, 149 13th Street, Charlestown, MA 02129, USA
[e] Department of Neuropsychiatric Disorders, Netherlands Institute for Neuroscience, an Institute of the Royal Netherlands Academy of Arts and Sciences, Meibergdreef 47, 1105 BA Amsterdam, The Netherlands
[f] Department of Radiology, MGH, 149 13th Street, Charlestown, MA 02129, USA
[g] Brigham & Women's Hospital (BWH), Department of Psychiatry, 1620 Tremont St. BC-3-34, Boston, MA 02120, USA
[h] BWH, Department of Medicine, Division of Women's Health, Connors Center for Women's Health & Gender Biology, 1620 Tremont St. BC-3-34, Boston, MA 02120, USA
[i] Department of Psychiatry, Harvard Medical School, Boston, MA, USA
[j] Department of Medicine, Harvard Medical School, Boston, MA, USA
[k] Department of Basic Medical Sciences, University of Arizona College of Medicine, 425 N. Fifth Street, Phoenix, AZ 85004, USA
[l] Department of Biomedical Sciences, Colorado State University, 1680 Campus Delivery, Fort Collins, CO 80523, USA

ARTICLE INFO

ABSTRACT

There is increasing evidence regarding the importance of the hypothalamus for understanding sex differences in relation to neurological, psychiatric, endocrine and sleep disorders. Although different in histology, physiology, connections and function, multiple hypothalamic nuclei subserve non-voluntary functions and are nodal points for the purpose of maintaining homeostasis of the organism. Thus, given the critical importance of hypothalamic nuclei and their key multiple roles in regulating basic functions, it is important to develop the ability to conduct in vivo human studies of anatomic structure, volume, connectivity, and function of hypothalamic regions represented at the level of its nuclei. The goals of the present study were to develop a novel method of semi-automated volumetric parcellation for the human hypothalamus that could be used to investigate clinical conditions using MRI and to demonstrate its applicability. The proposed new method subdivides the hypothalamus into five parcels based on visible anatomic landmarks associated with specific nuclear groupings and was confirmed using two ex vivo hypothalami that were imaged in a 7 T (7 T) scanner and processed histologically. Imaging results were compared with histology from the same brain. Further, the method was applied to 44 healthy adults (26 men; 18 women, comparable on age, handedness, ethnicity, SES) to derive normative volumes and assess sex differences in hypothalamic regions using 1.5 T MRI. Men compared to women had a significantly larger total hypothalamus, relative to cerebrum size, similar for both hemispheres, a difference that was primarily driven by the tuberal region, with the sex effect size being largest in the superior tuberal region and, to a lesser extent, inferior tuberal region. Given the critical role of hypothalamic nuclei in multiple chronic diseases and the importance of sex differences, we argue that the use of the novel methodology presented here will allow for critical investigations of these disorders and further delineation of potential treatments, particularly sex-specific approaches to gene and drug discoveries that involve hypothalamic nuclei.

© 2012 Elsevier Inc. All rights reserved.

Introduction

Traditionally it has been difficult to assess hypothalamic involvement in specific human behavior, affect, and cognition, given the difficulties of measuring this structure in vivo. However, current studies using in vivo structural and functional magnetic resonance imaging (s/fMRI) in humans have demonstrated potential hypothalamic roles in mood and arousal (Augustinack et al., 2005; Bao et al., 2005; Goldstein et al., 2010, 2005; Handa et al., 1994; Majdic and Tobet, 2011), and psychiatric

disorders (Goldstein et al., 2007). MRI offers advantages over traditional anatomy and histopathology, such as capabilities of in vivo measurement and monitoring of structure and function in healthy and clinical conditions. Using sMRI, a volumetric and topological analysis of the healthy hypothalamus with results matching those derived from traditional anatomy was used to differentiate schizophrenia patients, their first-degree relatives and healthy controls (Goldstein et al., 2007). Although this was an advance in the measurement and usefulness of the hypothalamus for understanding disease, there are a number of methodological and technological challenges that have hindered the progress of this line of research.

Anatomically, the human hypothalamus is a relatively small-sized structure, yet is considered a critical center for drive-related activities (such as feeding, defense and sexual behavior), endocrine and autonomic function (Baroncini et al., 2010; Saper et al., 2002; Swaab, 2003, 2004; Swanson, 2000). Currently, there is increasing evidence regarding the importance of the hypothalamus for understanding women's health and sex differences in relation to neurological, psychiatric, endocrine and sleep disorders. Although different in histology, physiology, connections and function, multiple nuclei of the hypothalamus subserve autonomic functions and are nodal points for the coordination of endocrine, emotional and somatic activities for the purpose of maintaining the organism within a healthy physiological equilibrium (i.e., homeostasis) (Saper et al., 2002; Swaab, 2003, 2004; Swanson, 2000). Overall, endocrine functions are primarily related to hypothalamic neuronal secretions into the median eminence to reach the anterior pituitary and direct projections to the posterior pituitary. Motivated behaviors are related to connections with limbic structures, such as the cingulate and parahippocampal gyri, amygdala and hippocampus. Somatic responses are associated with hypothalamic connections with somatic and visceral nuclei located within the brainstem and spinal cord (Koh and Ricardo, 1978; Saper et al., 2002). In fact, even specific nuclei within the hypothalamus, such as the paraventricular nucleus, have specific neuronal components associated with endocrine and autonomic functions (Herman et al., 2005; Stratton et al., 2011; Swaab, 2003, 2004; Swanson and Sawchenko, 1983). Hypothalamic regulation of the endocrine system plays a key role in the development of the sexual differentiation of the brain given the roles of hormones and genes on specific nuclei during particular gestational periods of development (Handa et al., 1994; Swaab, 2003, 2004; Tobet et al., 2009). This role has been demonstrated for many years in model animals and more recently in humans (Bao and Swaab, 2011; Goldstein et al., 2001; Raznahan et al., 2010). Thus, given the critical importance of hypothalamic nuclei and their key roles in regulating numerous functions, it is important to develop the ability to conduct in vivo human studies of anatomic structure, volumetry, connectivity, and function of hypothalamic regions represented at the level of its characteristic cell groups or nuclei. However, this level of structural analysis has not been currently achieved in hypothalamic MRI research. Traditional histology and immunohistochemistry has elucidated this level of analysis and thus serves as the "gold standard" to validate, guide and assist us in the MRI-based assessment and mapping of hypothalamic structure. Currently, the level of quantitative structural analysis that has been achieved in hypothalamic MRI research is measuring the volume of the entire hypothalamus using an approach of morphometric analysis (Goldstein et al., 2007). This is a different and complementary approach to the qualitative morphological characterization of the human hypothalamus for atlas generation using MRI (Baroncini et al., 2012).

The goals of the present study were two-fold: (1) develop a novel method of semi-automated, volumetric parcellation for the human hypothalamus that could be used to investigate clinical conditions using MRI, and (2) demonstrate the method's applicability. The new method extends previous work in which MRI was used to measure the entire hypothalamus as a single volumetric unit (Goldstein et al., 2007). In an effort to analyze quantitatively the human hypothalamus

at a more fine-grained level, the new method subdivides the hypothalamus into five measurable parcels (or parcellation units [PUs]) based on visible anatomic landmarks that are associated with specific nuclear groupings. To validate this method, two ex vivo hypothalami were imaged at high resolution in a 7 T scanner and then processed histologically. Imaging results were compared with the histological evaluation. The parcellation methodology was then used to analyze the hypothalami from 44 healthy adult subjects (26 men; 18 women) to derive normative volumetric data and assess sex differences in the hypothalamus in its entirety as well as in its five subdivisions and thus infer associations with more specific hypothalamic nuclear groupings.

Methods

Anatomic parcellation of the human hypothalamus using MRI and its validation

The hypothalamus is located in the diencephalon, ventrally to the thalamus and hypothalamic sulcus and surrounding the third ventricle. It extends rostrally from the anterior commissure and the lamina terminalis to the ventral tegmentum caudally just behind the mamillary bodies. Its ventral surface is exposed to the subarachnoid space and the cerebral spinal fluid covering a distance from the optic chiasm to the caudal edge of the mamillary bodies (see Fig. 1). The hypothalamus is constituted by at least 13 nuclei, which have a specific topography and maintain characteristic topographic relationships among them (intrinsic connections) and their neighboring structures (extrinsic connections). Using histological and immunohistochemical techniques, the visualization of the nuclei is feasible. However, this is not currently possible using MRI given technological challenges such as spatial resolution. Thus to reliably segment the hypothalamus, it is necessary to follow conventions with respect to anatomic morphologic landmarks that consistently are identifiable using (Goldstein et al., 2007).

In the present method, the hypothalamus was first segmented as a whole in the coronal plane [as described by Goldstein et al. (2007)] using a semi-automated morphometric method based on 1.5-T MR images. Briefly, in the rostrocaudal dimension anteriorly, semi-automated segmentation of the hypothalamus began by convention at the coronal section containing the anterior-most tip of the anterior commissure (AC) and the optic chiasm (OC), which is reliable. The preoptic hypothalamus would be present on both sides of the third ventricle below the AC and above the OC. More caudally, at the level of the interventricular foramen of Monro and amygdala, the anterior part of the hypothalamus is observed on both sides of the third ventricle, and its lateral border at this level is demarcated by the lateral extent of the optic tracts as the optic chiasm bifurcates caudally. At a more caudal coronal level passing through the anterior thalamus, the amygdala and anterior hippocampus, the tuberal part of the hypothalamus is observed on each side of the third ventricle and segmented above the infundibular stalk and below the hypothalamic sulcus of Monro (Déjerine, 1895; Nieuwenhuys et al., 2008) and posterior limb of the internal capsule. Laterally, the hypothalamic border extends to the posterior limb of the internal capsule and the vicinity of the globus pallidus. Further caudally, the posterior part of the hypothalamus, including the mamillary bodies, is segmented. The lateral border of the hypothalamus is principally with the internal capsule, globus pallidus, and cerebral peduncle, whereas the medial border is at the midline of the hemisphere opposing the contralateral posterior hypothalamic nucleus and mamillary body. Its superior border is with the third ventricle and the diencephalic fissure. This border is prompted by white matter fibers above the mamillary body and lateral to the third ventricle, which belong principally to the mamillothalamic tract. The inferior border of the posterior hypothalamus is the hemispheric margin.

Subsequently, the hypothalamus was subdivided manually into five parcellation units (PUs) based on landmarks directly visible on
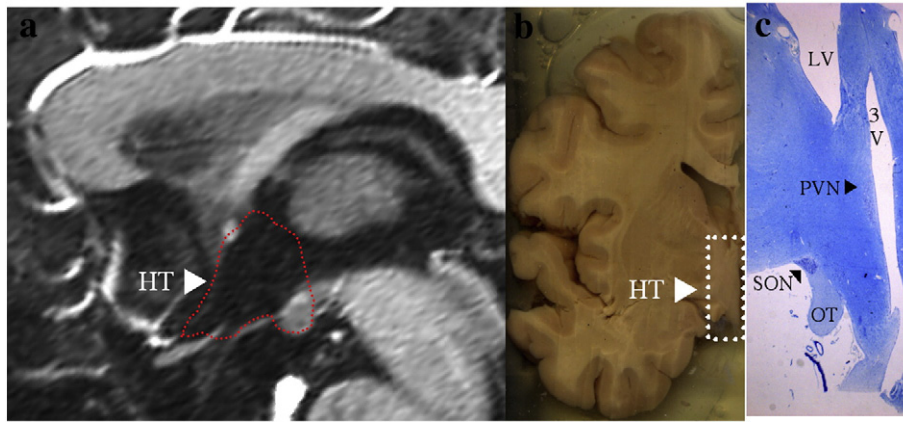
Fig. 1. Location of human hypothalamus in vivo MRI and paraventricular and supraoptic nuclei by histology. The location of the human hypothalamus (HT) is shown in a mid-sagittal T1 weighted MRI section within the area surrounded by the dashed red outline as projected in the third ventricle (a) and in a coronal section of a grossly dissected human hemisphere within the area surrounded by the dashed white rectangle (b). In (c), the paraventricular nucleus (PVN) and the supraoptic nucleus (SON) are indicated by black arrowheads in a coronal histological section stained with thionin. OT = optic tract, LV = lateral ventricle, 3 V = third ventricle.

the MRI images. These are the anterior–superior (a-sHyp) and anterior–inferior (a-iHyp), superior tuberal (supTub), inferior tuberal (infTub) and posterior (posHyp) hypothalamic PUs. Given that the lateral borders of these PUs were outlined during the segmentation of the hypothalamus as a whole, this more fine-grained subdivision was related only with the definition of their anterior–posterior and superior–inferior borders. The anterior hypothalamic PUs (i.e., a-sHyp and a-iHyp) extended from the anterior most tip of the anterior commissure (AC) to the anterior most tip of the infundibulum in the anterior-posterior dimension (i.e., the Y axis). The tuberal PUs (i.e., supTub and infTub) extended from the anterior most section containing infundibulum to the coronal section just anterior to the mamillary body (MB). The section containing the anterior most tip of MB was the anterior border of posHyp and was included in posHyp. The posHyp PU extended caudally until it included the entire MB. The border between the superior and inferior anterior PUs was set at the superior most level of the floor of the substantia innominata (Nieuwenhuys et al., 2008) or the anterior and lateral perforated substance (Duvernoy, 1999) and likewise between the superior and inferior tuberal PUs (see Fig. 2). The segmentation of each hypothalamus and its five subdivisions into five parcels required approximately 1 h of a trained investigator's time. This schema of morphometric parcellation of the human hypothalamus is similar to the classical approach of subdivision of this structure. That is, it parcellates the hypothalamus into three general parcels (anterior, tuberal and posterior) as has been portrayed in neuroanatomy textbooks (Nolte, 2009; Parent, 1996).

Confirmation of PUs in ex vivo samples using MRI and histology

Two formalin-fixed ex-vivo hypothalamic samples were provided by one of the co-authors (D.S.) from the Netherlands Brain Bank (NBB). There are more than 2,000 donors (both with and without brain disorders) to the NBB collection of hypothalami. NBB donors gave permission for brain autopsies so that the physical material and clinical files could be used for research purposes. Data on these donors have been related to a substantial number of findings in the hypothalamus published in multiple papers on structural and molecular differences in relation to age, sex, gender identity, sexual orientation, and diseases [see Swaab (2003, 2004)]. Hypothalami from two donors were used in this study. They were two men: age at autopsy 29 and 51 years, brain weight 1060 and 1310 g, postmortem interval <17 h, and causes of death, congestive heart failure and cardiac failure, respectively. Each hypothalamic sample contained right and left hypothalamus in their entirety and measured approximately 23 mm, in the medio-lateral (X), 14 mm in the anterior posterior (Y), and 24 mm in the vertical (Z) dimensions.

Scanning of the tissue samples was performed using a 7-T MRI scanner with a custom-made small single-channel coil (with inner diameter = 30 mm). Six scans were completed, two at each of the following flip angles: 10°, 20° and 30°, from which quantitative T1 and PD values were calculated at each voxel by solving the steady-state FLASH equation. Due to the high TE, the native images were T2* weighted. Each scan lasted 6,513 s (1 h, 48 min, 33 s) and was repeated twice. Thus total acquisition time was 39,078 s (10 h, 51 min, 18 s). The sequence was a 3D spoiled gradient echo (FLASH) with the following parameters: TR = 53 ms; TE = 25 ms; bandwidth = 30 Hz/pixel; FOV = 35×35 mm^2; matrix = 384×384; 320 consecutive slices (no gap); voxel size .09 mm (90 μm) isotropic. After scanning, each MR image data set was saved and transferred to DVD and maintained in duplicate copy. These two high-resolution datasets were subdivided into the five parcellation units (PUs) following the method described in the "Anatomic parcellation of the human hypothalamus using MRI and its validation" section.

After MRI acquisition, these two hypothalami were processed histologically, (i.e., embedded in paraffin, sectioned, and stained for Nissl substance and vasopressin by D.F.S). Every 100th (6 μm thick) section throughout was selected for staining from a series of 800 sections that constituted the entire hypothalamic tissue block. Thus the tissue block was 4.8 mm thick and the representative 14 sections used were chosen at equal intervals between them within the block of tissue. Deparaffinized sections were stained for Nissl substance using thionin to serve as the gold standard guiding MRI anatomical interpretations and helping elucidate precisely the topography of nuclei within the hypothalamic parcellation units.

The stained sections were digitized and compared with their corresponding sections of the MRI representations. The MRI datasets were aligned to the tissue samples following two procedural steps. First, scanning of the tissue block was done in a custom-made coil that allowed its positioning in a comparable fashion to its histological processing. Precisely, the plane of scanning was as parallel as possible to the plane of sectioning of the tissue block after its parafinization. Second, prior to parcellation of the histological and MRI datasets of each tissue block, the digitized histological data were visually inspected and the 3-D MRI datasets were adjusted to match the sections as much as possible. Given that alignment was achieved adequately, the fact that the same tissue sample was first imaged and then processed histologically, the observations of the MRI and histological data were directly comparable. Although co-registration of ex vivo histologically processed tissue, namely parafinized and stained, may lead to errors in alignment with the same tissue prior to be processed, we think that the alignment obtained herein was
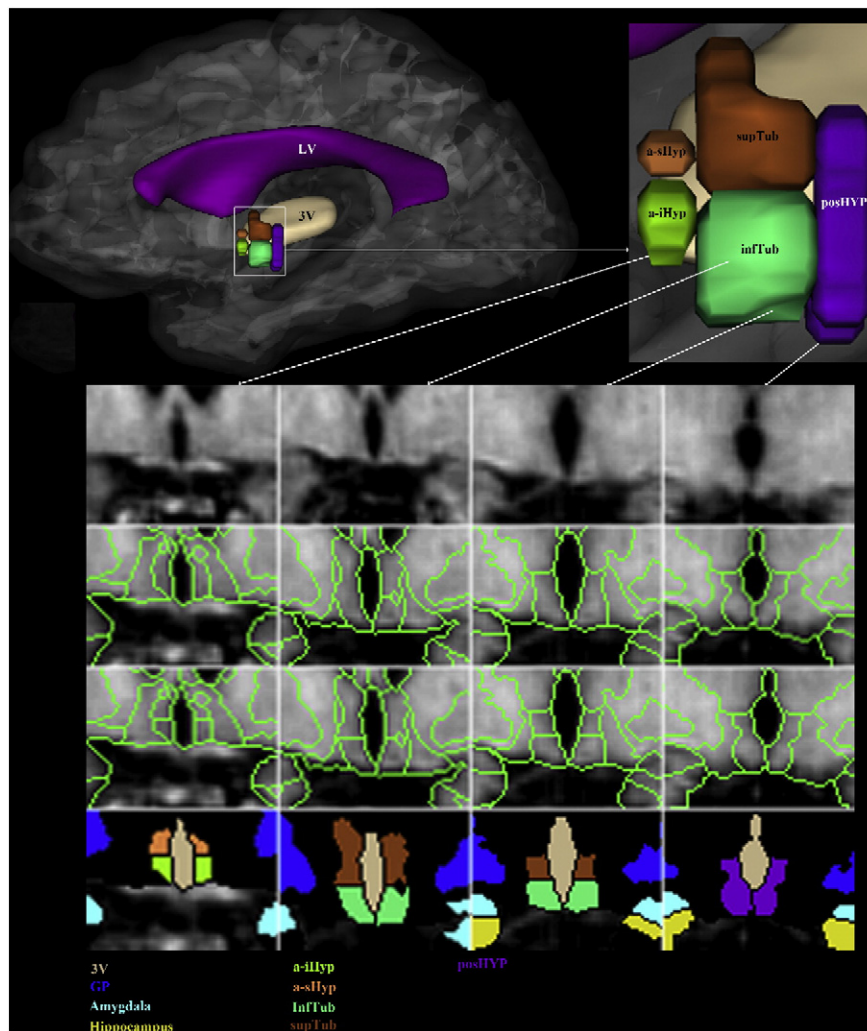
Fig. 2. Parcellation method of the human hypothalamus in vivo using 1.5 T MRI. In a lateral view of the medial aspect of the cerebrum, the left hypothalamus is shown within a rectangle, which is then illustrated magnified in the upper right corner of the figure. In the lower part of the figure, a set of 16 cells represents the method of parcellation used for the hypothalamus. The upper row shows four raw coronal images of T1-weighted MRI in which the hypothalamus is present in an anterior–posterior progression from left to right. The second row shows segmentation of the hypothalamus as a whole as described in Goldstein et al. (2007). In the third row the fine-grained parcellation of the hypothalamus has been applied. The result of this parcellation is five different parcellation units, which are color-coded in the bottom row. Abbreviations: a-iHyp = anterior–inferior hypothalamus, a-sHyp = anterior–superior hypothalamus, GP = globus pallidus, infTub = inferior tuberal hypothalamus, posHyp = posterior hypothalamus, supTub = superior tuberal hypothalamus, LV = lateral ventricle, 3 V = third ventricle.

satisfactory. This approach has been used previously for validating results obtained with high-field imaging in humans for cortical regions such as entorhinal cortex (Augustinack et al., 2005) and cerebral cortex (Fischl et al., 2008). Furthermore, aside from the use of ex vivo tissue as proof of principle, it provides critical information as to the voxel size necessary to conduct high field imaging of hypothalamic nuclei, such as the paraventricular nucleus. To apply this method to 1.5 T data, we compared the 1.5 T dataset to the 7 T data and their corresponding histological representations (see Fig. 5 and "Parcellation of 7 T MRI datasets and comparison to their own histology" section).

Normative volumetric measurements and sex differences in the adult human hypothalamus

We measured the hypothalamus by applying the anatomically confirmed parcellation method (described in 2.1.), which measures the total hypothalamus and its five PUs, in 44 healthy subjects (26 males and 18 females). MRI scans were initially acquired with a 1.5-T General Electric Signa scanner. Contiguous 3.0-mm coronal spoiled gradient echo images of the entire brain were obtained by using the following parameters: TR = 40 msec, TE = 8 msec, flip angle = 40°, FOV = 24 cm, matrix = 256 × 256, and NEX = 1. All scans

acquired in the in vivo condition were normalized with respect to a standard coordinate system prior to image analysis (Filipek et al., 1994). The result was a new set of reformatted, coronal images in the standard orientation, sampled at the same resolution (in-plane and slice) as the original data acquisition.

Our method for hypothalamic parcellation (described in 2.2.) was applied to brain images of healthy subjects, shown in detail in Fig. 2a–o. Subjects were a healthy community sample from the Boston area recruited for two previous studies of ours (NIMH R01 MH63951 and MH56956) and acquired using the same 1.5 T Siemens scanner and MRI acquisition protocol. Subjects consisted of 26 men and 18 women, 42 ± 11.5 and 38 ± 9.6 years old, respectively. They were all Caucasian, right-handed, with similar socioeconomic backgrounds [education (mean = 14.7 ± 2.3 and 14.6 ± 2.3 years, respectively)], and general level of intelligence (mean = 113.2 ± 12 and 111.2 ± 15, respectively), and thus not significantly different by sex. Subjects were systematically interviewed diagnostically and assessed as having no Axis I psychiatric disorders or major health conditions. Inter-rater reliability for total hypothalamus assessed by intra-class correlation coefficient (ICC) for 10 brains by two raters was strong at 0.81 for right and left hypothalamus, as previously shown (Goldstein et al., 2007). There were excellent inter-rater reliabilities for the five PUs (ICCs = 0.99) and intra-rater
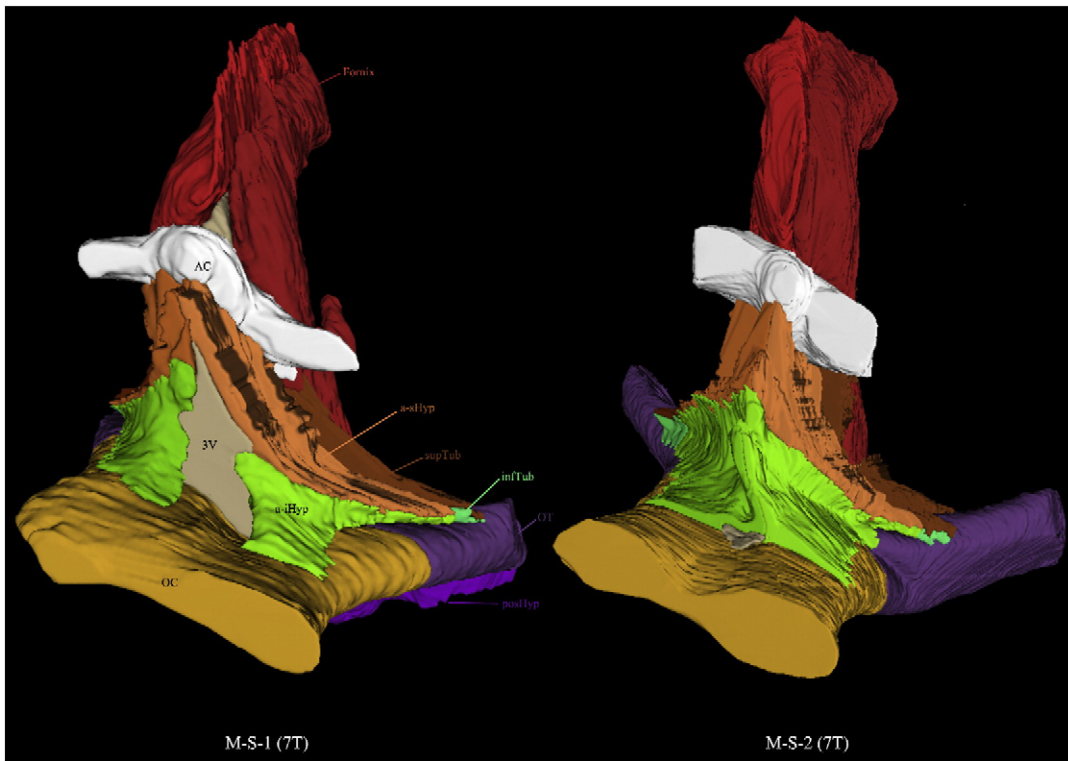
Fig. 3. 3-D reconstructions from segmentation of two ex vivo 7 T MRI of the human hypothalamus. Each hypothalamus was parcellated into five distinct parcellation units. Abbreviations: AC = anterior commissure, a-iHyp = anterior–inferior hypothalamus, a-sHyp = anterior–superior hypothalamus, infTub = inferior tuberal hypothalamus, OC = optic chiasm, posHyp = posterior hypothalamus, supTub = superior tuberal hypothalamus.

reliability for the five PUs (conducted by D.B.) (ICCs = 0.90). Analyses of variance were conducted to test for sex differences in regional hypothalamic volumes for total, posterior, tuberal, and anterior PUs, controlled for cerebrum size, given that men have a larger cerebrum than women (Goldstein et al., 2001). Significance threshold was set at $p < 0.01$ to control for multiple comparisons.
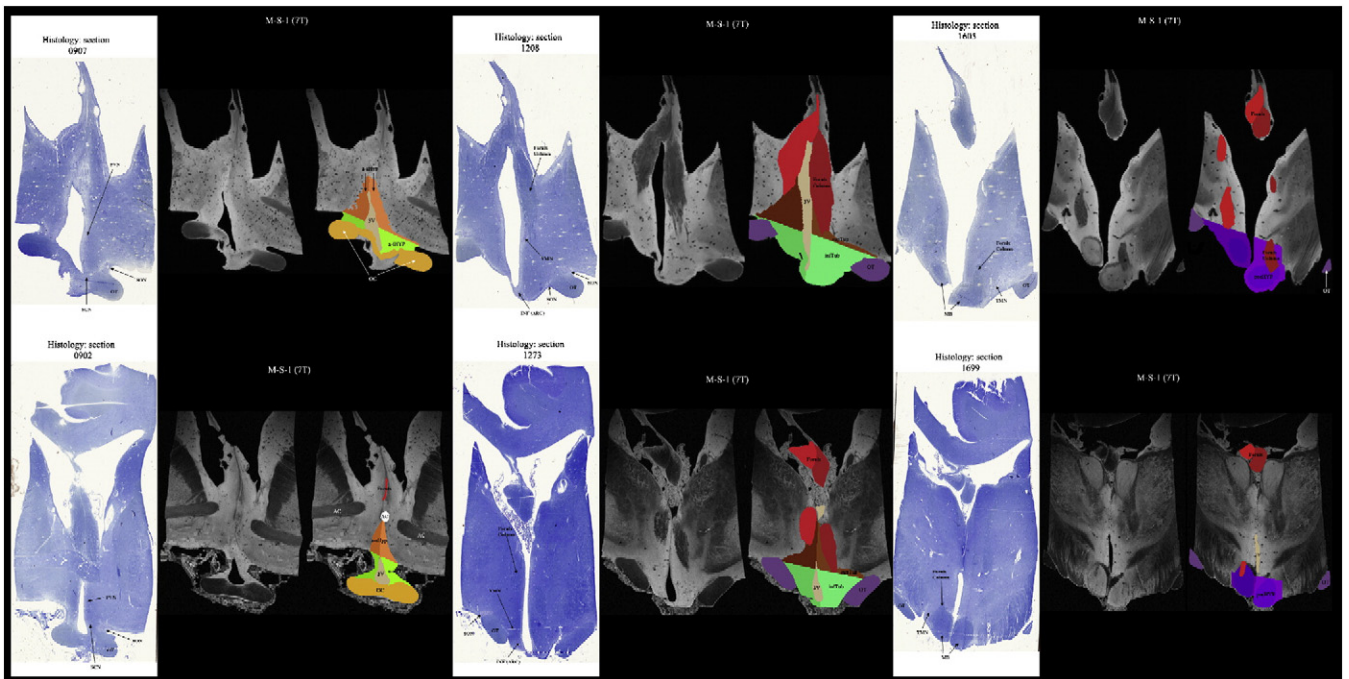
Fig. 4. Comparison and matching of ex vivo 7 T MRI against its own histology. In this comparison of the in-vivo MRI datasets with the ex-vivo MRI datasets and their corresponding histological representations, we were able to compare and match the 1.5 T in vivo images with the 7 T MRI ex vivo images and their histology. Abbreviations: AC = anterior commissure, a-iHyp = anterior–inferior hypothalamus, a-sHyp = anterior–superior hypothalamus, INF(ARC) = infundibular (or arcuate) nucleus, infTub = inferior tuberal hypothalamus, MB = mamillary body, OC = optic chiasm, OT = optic tract, posHyp = posterior hypothalamus, PVN = paraventricular nucleus, SCN = suprachiasmatic nucleus, SON = supraoptic nucleus, supTub = superior tuberal hypothalamus, TMN = tuberomamillary complex, VMN = ventromedial nucleus.

Table 1
Parcellation units of the hypothalamus and associated nuclei.

Parcellation unit (PU)	Nuclei
a-sHyp	preoptic area; diagonal band of Broca (DBB); sexually dimorphic nucleus of the preoptic area (SDN or INAH-1); paraventricular nucleus (PVN)
a-iHyp	DBB; nucleus basalis of Meynert (NBM); suprachiasmatic nucleus (SCN); supraoptic nucleus (SON)
supTub	PVN; dorsomedial nucleus (DMN); lateral hypothalamus
infTub	NBM; SON; infundibular nucleus (INF) (this is the same as the rodent arcuate (ARC) nucleus); ventromedial nucleus (VMN); nucleus tuberalis lateralis (NTL); tuberomamillary complex (TMN)
posHyp	mamillary body (including medial and lateral mamillary nuclei); lateral hypothalamus; TMN

Abbreviations: a-iHyp = anterior–inferior hypothalamus, a-sHyp = anterior–superior hypothalamus, GP = globus pallidus, infTub = inferior tuberal hypothalamus, posHyp = posterior hypothalamus, supTub = superior tuberal hypothalamus.

Results

Results are organized in the following way: (1) parcellation of 7 T MRI datasets and their comparison against their own (ex vivo) histology to determine hypothalamic nuclei within each parcellation unit; (2) comparison of 7 T ex vivo to in vivo 1.5 T data; and (3) application of the novel method to hypothalamic volume assessment of 1.5 T MRI data in a healthy normative sample of men and women.

Parcellation of 7 T MRI datasets and comparison to their own histology

Parcellation of the 7 T datasets was carried out satisfactorily as shown in Fig. 3. To this end, two postmortem hypothalami were segmented as a whole and subdivided into the five parcellation units (PUs) per hemisphere. The total postmortem hypothalamus measured 835.2 mm^3 on average (890.5 mm^3 and 779.8 mm^3 respectively), which is approximately 8% smaller than the observed average volume of the total hypothalamus as observed using the MRI methodology in vivo. Furthermore, comparison of histology to 7 T MRI allowed us to identify hypothalamic nuclei in the histological preparations and to determine where the nuclei belong within the PUs of the hypothalamus. Thus, in *a-sHyp*, there was preoptic area, diagonal band of Broca (DBB), sexually dimorphic nucleus of the preoptic area (SDN or INAH-1) and paraventricular nucleus (PVN). In *a-iHyp*, there was DBB, nucleus basalis of Meynert (NBM), suprachiasmatic nucleus (SCN) and supraoptic nucleus (SON). In *supTub*, there was PVN, dorsomedial (DMN) and lateral hypothalamus. In *infTub*, there was NBM, SON, infundibular (INF) (same as arcuate nucleus (ARC) in rodents), ventromedial (VMN), nucleus tuberalis lateralis (NTL) and tuberomamillary nucleus (TMN). Finally, in *posHyp*, there was mamillary body (including lateral and medial mamillary nuclei), lateral hypothalamus and TMN. Fig. 4 and Table 1 show the validation of the hypothalamic parcellation comparing ex-vivo 7 T MRI versus its own histology (see Fig. 4 and Table 1). Compared to existing atlases [see e.g., Mai et al. (1997) and Baroncini et al. (2012)] and classifications (Nolte, 2009), our results that follow the established schema of Swaab (2003) are similar.

Comparison of 7 T ex vivo and 1.5 T in vivo datasets

Subsequently, there was established comparability of the MRI parcellation method using ex-vivo, histologically validated high resolution 7 T datasets and then lower resolution in-vivo 1.5 T datasets. Results were satisfactory, as shown in Fig. 5 using 2-D coronal representations and 3-D reconstructions. This was necessary to apply the method to

1.5 T data and demonstrated applicability of this method to lower resolution datasets, which are routinely used in MRI clinical practice.

Finally, the methodology was applied to a community sample of 44 healthy men and women, a sample unselected for illness or any particular exposures to investigate sex differences in specific hypothalamic areas. As seen in Table 2, results showed that men compared to women had a larger total hypothalamus corrected for brain size, a similar difference for both hemispheres [$F(1, 42) = 10.75$, $p < 0.01$]. This difference was primarily being driven by the tuberal region [$F(1, 42) = 6.54$, $p = 0.01$], with the sex effect size (ES) being largest in the superior tuberal (ES = 0.70) and to a lesser extent the inferior tuberal (ES = 0.62) in both hemispheres.
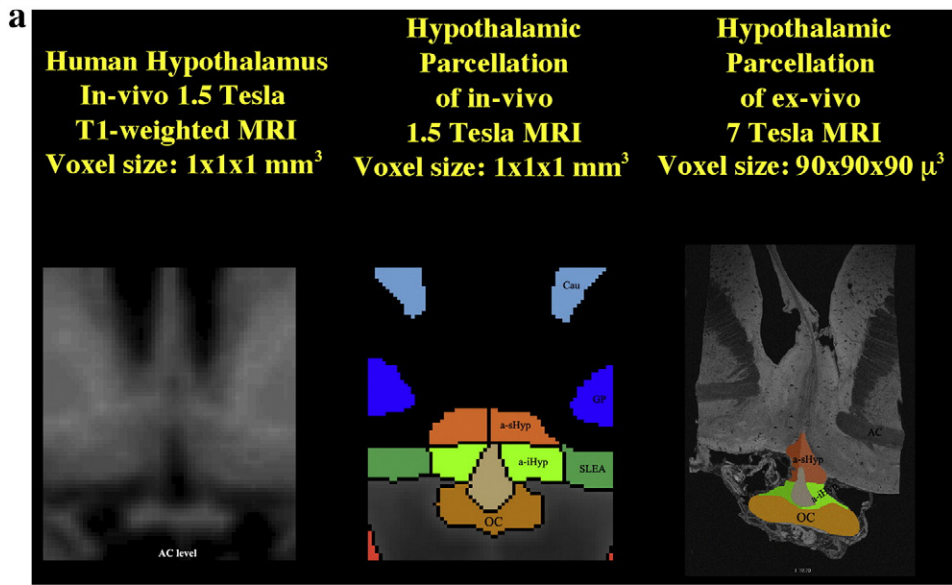
Discussion

This study created and confirmed a novel method for the study of the human hypothalamus in vivo. The hypothalamus was subdivided in five parcels and the analysis demonstrated the neurobiological meaning of each one of these subdivisions by identifying the structures (i.e., the nuclei) that are present within them. This was achieved by comparing imaged ex vivo human hypothalami with their histological data. The importance of this advance in hypothalamic research in the field of human neuroimaging lies in the ability of future studies to ascertain influences of nuclear sizes based on MR images obtained by standard protocols using 1.5 or 3 T scanners.
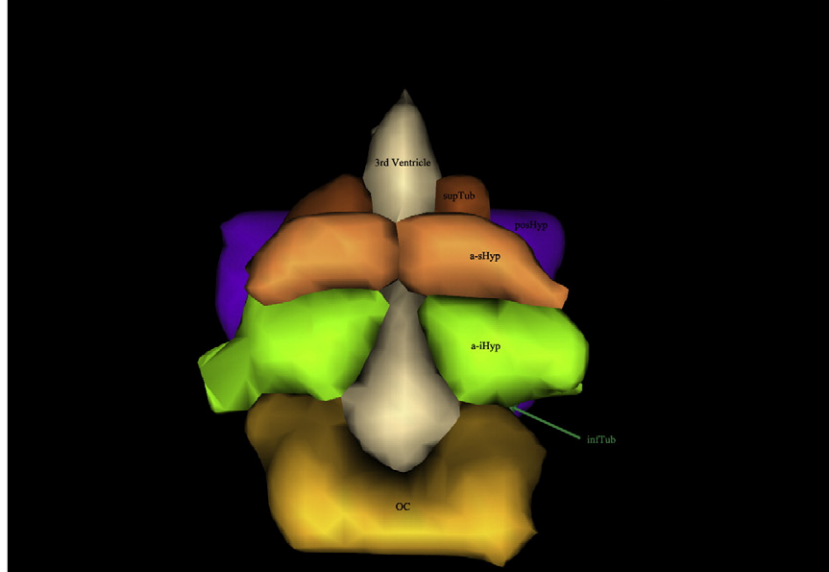
The hypothalamus is a critical brain structure in the survival of the individual, which is central in regulating affect, autonomic and endocrine functions, immune responses, as well as thirst, hunger, body temperature, sleep, mood, sex drive, rage and the stress response. Activation of the hypothalamic-pituitary–adrenal (HPA) axis is a typical response to stress. A primary event for HPA axis activation is the secretion and further synthesis of corticotropin-releasing hormone (CRH) by cells of the PVN. CRH in turn stimulates the release of adrenocorticotropic hormone (ACTH) from the adenohypophysis. ACTH transported via the bloodstream stimulates the adrenal glands to produce and secrete corticosteroids, such as cortisol, and sex steroid hormones (estradiol and androgens), which in turn inhibit further secretion of CRH. This system plays a key role in regulating arousal, neuroendocrine responses and affect, and has demonstrated significant sex differences in functioning at the MRI and postmortem levels (Bao and Swaab, 2007; Goldstein et al., 2010). Hypothalamic nuclei, such as the PVN and ventromedial nucleus (VMN), are involved in the regulation of HPA hormones and cytokine release, have connections with brainstem regions, and are responsible for autonomic nervous system (ANS) function, adrenal and ovarian function and aggression, sexual and maternal behaviors (Handa et al., 1994; Swaab, 2003, 2004; Tobet et al., 2009). In the present study, sex differences were noted in the size of hypothalamic regions, particularly the tuberal region that includes the INF, PVN, VMN, LHA and SON. In fact, model animal work on the hypothalamus and its sexual differentiation and importance for understanding multiple behaviors has been ongoing for >50 years, and has identified sex differences in these nuclei structurally and/or with their associated functions (Bao and Swaab, 2011; Tobet and Fox, 1992). Thus, the literature and our previous work underscore the importance of hypothalamic nuclei, such as the PVN, the necessity of their in vivo imaging in clinical populations, and the importance of sex differences in the brain associated with hypothalamic regions and their functions.

Currently, there are very few in vivo studies of the human hypothalamus (Baroncini et al., 2012) given the difficulty to image this structure. Most work on the human hypothalamus is based on human and experimental postmortem studies or clinical endocrine studies, which have not utilized neuroimaging techniques and are devoid of structural or

Fig. 5. Comparison of parcellation of 1.5 T in vivo with 7 T ex vivo hypothalamus. Comparison between parcellation results of 1.5 T in vivo and 7 T ex vivo hypothalamic datasets in 2-D coronal representations (5a) and 3-D reconstructions (5b, c). Abbreviations: a-iHyp = anterior–inferior hypothalamus, a-sHyp = anterior–superior hypothalamus, infTub = inferior tuberal hypothalamus, OC = optic chiasm, posHyp = posterior hypothalamus, SLEA = sublenticular extended amygdala, supTub = superior tuberal hypothalamus.

a

Human Hypothalamus In-vivo 1.5 Tesla T1-weighted MRI Voxel size: 1x1x1 mm³

Hypothalamic Parcellation of in-vivo 1.5 Tesla MRI Voxel size: 1x1x1 mm³

Hypothalamic Parcellation of ex-vivo 7 Tesla MRI Voxel size: 90x90x90 µ³

b **In-vivo 1.5 Tesla 1 mm³ 3-D reconstruction of Hypothalamus**

c **Comparison between in-vivo and ex-vivo MRI results**

In-vivo 1.5 Tesla MRI

Ex-vivo 7 Tesla MRI
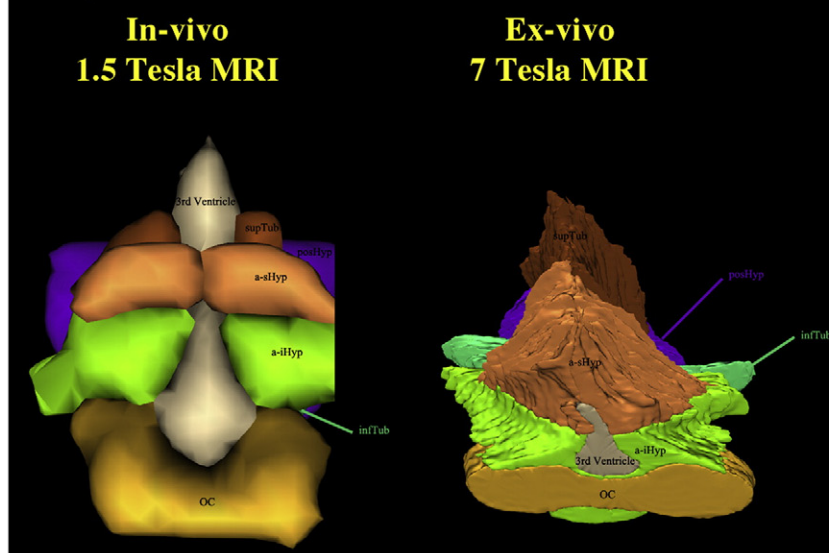
Table 2
Sex differences in hypothalamic parcellation units (cm³) in the healthy brain.

Areas	Males ($N=26$)		Females ($N=18$)	
	Mean (cm³)	SD (cm³)	Mean (cm³)	SD (cm³)
L. Posterior Hyp	.11	.04	.10	.05
R. Posterior Hyp	.12	.04	.10	.04
Total Posterior Hyp	.23	.08	.20	.08
L. Superior-Tuberal Hyp	.10	.04	.07	.03
R. Superior-Tuberal Hyp	.11	.04	.08	.04
L. Inferior-Tuberal Hyp	.13	.05	.10	.05
R. Inferior-Tuberal Hyp	.14	.05	.11	.06
Total Tuberal Hyp*	.48	.15	.39	.16
L. Anterior–Superior Hyp	.05	.02	.06	.02
R. Anterior–Superior Hyp	.06	.03	.06	.03
L. Anterior Inferior Hyp	.04	.02	.05	.02
R. Anterior–Inferior Hyp	.05	.03	.06	.03
Total Anterior Hyp	.21	.09	.23	.07
Total Left Hyp*	.43	.06	.38	.07
Total Right Hyp*	.48	.06	.41	.08
Total Hypothalamus*	.91	.11	.79	.14

Notes: Standard deviations are presented in italics next to means. Significant sex differences ($p \leq 0.01$) are indicated with an asterisk (*). Sex differences were only tested for "Total" measurements (in bold). Abbreviations: Hyp = hypothalamus, L = left, R = right.

functional brain information. Furthermore, in vivo investigations are necessary to correlate structural hypothalamic alterations with behavioral, clinical and genetic phenotypes. Most current MRI methods allow in vivo measurements of the hypothalamus to the extent of the entire structure (Goldstein et al., 2007), except for a recent study by Baroncini et al. (2012). The latter showed the association between histological and MRI data for the human hypothalamus allowing for a localization of nuclei at a qualitative level of morphological analysis (Baroncini et al., 2010, 2012).

To construct a quantitative MRI-based method that is biologically meaningful, it is necessary to identify and measure individual hypothalamic nuclei or nuclear groups associated with the MRI-based anatomy as presented in the current study. A unique advantage of our approach is that it can be applied to commonly acquired images of living tissue, such as with 1.5 or 3 T MR scanners, allowing for investigations of clinical populations. Recently, this approach has been used to study in vivo brain structure in humans using MRI for the hippocampus [e.g., Cho et al. (2008)]. These studies share the concept of comparing living human tissue observed by MRI with postmortem human tissue to validate and establish a methodology for use in living humans. Recently, Baroncini et al. (2012) provided an atlas of the human hypothalamus associating the histology of this structure with 1.5 T MRI data. Given that the direct identification of hypothalamic nuclei is not feasible, the creation of an atlas is relevant to establish a relationship between the hypothalamic PUs of our parcellation methodology with hypothalamic nuclei. To this end, we used the schema proposed by Swaab (2003) rather than Baroncini et al. (2012), and parcellated ad hoc 7 T ex vivo hypothalamic datasets and correlated them with their own histology. Importantly, besides the fact that histological processing was performed by one of the authors (DFS) following his established schema, hypothalamic nuclei were identifiable by high-resolution 7 T MRI, and these same MRI datasets were parcellated into the five PUs proposed in our method. Thus, the unique approach in the study presented here was that the same hypothalami were used for high resolution 7 T MRI scanning, MRI-based hypothalamic parcellation, histology-based hypothalamic parcellation and histological analysis of the hypothalamic nuclei. This offered an anatomical verification of our methodology and provided a means of anatomical validation.

A few limitations should be considered with respect to this study. One limitation relates to the method for validating the system by in vivo to ex vivo comparison. Aside from the strictly technical differences between the two categories of materials and procedures involved for in vivo MRI and ex vivo MRI and histology, there are

important conceptual considerations surrounding the notions of qualitative and quantitative neuroanatomy and, ultimately, what is considered methodologically valid in quantitative MRI analysis of the hypothalamus. Historically, most analyses and discoveries in neuroanatomy and histology have been qualitative, either demonstrating the existence of a structure or showing and describing its morphology. Nevertheless, this level of explanation does not fully address several questions such as interindividual variability and covariance of structures in the brain, which have important implications in understanding brain organization (Makris, 1999). In contrast, this is only feasible by quantitative approaches, such as MRI-based brain volumetrics, a framework within which "(1), regularities in relative variation of volumes with respect to mean volume of a structure are viewed as systematic manifestations of the rules of histogenetic process" and "(2), regularities in the relative strength of correlation of volumes of structures are suggested to reflect constraints which serve systematically the requirements of neural systems operation." (Caviness et al., 1999). Thus qualitative and quantitative approaches are complementary in neuroanatomy. Furthermore, the recent advances in imaging technology have facilitated the development of morphometric methodologies and the advancement of computational neuroanatomy in an unprecedented way. Finally, in quantitative MRI-based volumetry tradition, a methodology has been considered valid when it complies with certain standards of reliability and anatomical accuracy. These standards are empirical and have evolved over time in the field of MRI-based brain morphometry [see e.g., (Bouix et al., 2007; Jovich et al., 2009; Makris et al., 2005, 2006)].

Fixation and tissue processing procedures such as parafinization and staining affect the tissue size and structure in several ways. The typical net result of the size changes is tissue shrinkage, with swelling occurring relatively rarely (e.g., osmium fixation procedures). The processes that lead to tissue size alteration due to its preparation for histological analyses mainly involve dehydration as well as precipitation of proteins and polymerization. As has been reported by others (Braitenberg and Schuz, 1998), tissues could show alterations from 42% to 80% of their original volume due to fixation and staining effects (Drenhaus et al., 1986; Mouritzen Dam, 1979; O'Kusky and Colonnier, 1982; Romeis, 1968; Schuz and Palm, 1989; Stephan, 1960; Werner and Winkelman, 1976). Discrepancies in measurement between the histologically processed sections with the MRI-based results of these tissue blocks, were anticipated due to the effects of parafinization and staining procedures on the size of the tissue, given these tissue blocks were processed histologically, i.e., parafinized, sectioned and stained after being imaged. Another challenge has been co-registration of stained sections with the MRI ex vivo corresponding slices. As elaborated upon in the body of the method section herein, we addressed this problem to minimize errors in alignment. Bearing these caveats in mind, we think our method was validated satisfactorily compared with how others in the field have approached this (Augustinack et al., 2005; Baroncini et al., 2012; Cho et al., 2008).

Another set of limitations relate to translating information derived from ex vivo analyses to in vivo ones. Unfortunately, most technological advances in the postmortem imaging domain, and the information derived from such comparison, cannot be directly transferable to the in vivo MRI domain. This incomparability is due to a number of limitations on both sides. Physiologic motion in living tissue deteriorates the image resolution, motion that is not present in postmortem tissue. Further, the structure of postmortem tissue is altered due to fixation, which changes the interactions of the water molecules and their surrounding tissue. Fixatives, such as formaldehyde, produce covalent bonding, cross-linking or precipitation among bio-macromolecules (such as proteins), thus changing the interaction between molecular entities. This bonding affects the T1 and T2 relaxation times of the water proton and changes the appearance of the signal and the acquired image. These interactions also change the contrast mechanisms of the tissue water in the ex vivo fixed tissue as compared to in vivo tissue,

thus the resulting signal and images will be different. The major problem for the hypothalamus is that MRI contrast is mainly based on myelin versus gray matter. In the hypothalamus, the nuclei are not surrounded by myelinated fibers resulting in contrast attenuation. This underscores the value of the technique presented here and our approach to validation. It should be noticed that in this study the focus was to develop an MRI-based volumetric method of the human hypothalamus. Even if the level of correspondence of the individual nuclei was qualitative and could not be ascertained with certainty and thus anatomical accuracy was limited, the level of reliability of the in vivo MRI-based measures was very high. Overall, this method offers a significant increment in our knowledge and our capabilities of conducting MRI-based volumetric research with the human hypothalamus in healthy and clinical conditions. Future studies should consider the implementation of multi-modal structural MRI (e.g., T1-, T2-weighted and diffusion MRI) to parcellate the human hypothalamus and its anatomical connections (Lemaire et al., 2011). Furthermore, future studies can generate probabilistic atlases based on large sample sizes of ex vivo hypothalami to improve the accuracy of identifying individual hypothalamic nuclei in imaging studies.

Although there are technological challenges to create the ideal method, there is a critical need from the standpoint of understanding the role of the hypothalamus in multiple chronic diseases. Hypothalamic nuclei are key regulators of autonomic and endocrine functions, mood and stress response, and are implicated in psychiatric and general medical disorders, and particularly those with known sex differences in incidence. At the postmortem level, the PVN is enlarged in patients with major depressive disorder (MDD), in particular PVN neurons that are dense in CRH and estrogen receptor (ER)α (Bao et al., 2005). At the in vivo imaging level, premenopausal women with MDD show brain activity deficits in anterior hypothalamus, related to gonadal hormone deficits (Holsen et al., 2011) and autonomic nervous system dysregulation (Holsen et al., 2012). Further, our recent animal studies on models of prenatal stress and risk for sex differences in depression-related behaviors and brain outcomes demonstrated sex-specific effects of GABA signaling in PVN development (McClellan et al., 2010; Stratton et al., 2011) and excess glucocorticoid exposure (Zuloaga et al., 2011). In schizophrenia, we identified structural abnormalities in the anterior hypothalamus, suggestive of PVN abnormalities in women (Goldstein et al., 2007). Furthermore, in healthy women using functional MRI, we demonstrated that sex differences in anterior hypothalamus, including PVN and VMN, under stress, were dependent on gonadal hormone changes over the menstrual cycle (Goldstein et al., 2005, 2010). These findings suggest that an understanding of the role of hypothalamic nuclei in MDD, schizophrenia, ANS regulation, and other disorders, will contribute to understanding sex differences in the incidence of these disorders (Goldstein, 2006; Goldstein et al., 2012). Thus, the use of the novel methodology presented here will allow for critical investigations of these disorders and the further delineation of potential treatments, particularly sex-specific approaches to gene and drug discoveries that involve the hypothalamus.

Conclusions

Here we have presented a unique and innovative methodology for the segmentation of the human hypothalamus, which subdivides the hypothalamus into five parcels based on visible anatomic landmarks associated with specific nuclear groupings. We provided an initial validation of the method using two ex vivo hypothalami imaged in a 7-T scanner and processed histologically, and applied it to 44 healthy men and women, comparable on age, handedness, ethnicity, and socioeconomic status. We reported normative volumes for men and women, and demonstrated significant sex differences in the overall size of the hypothalamus (similar across hemispheres, relative to overall cerebrum size) that was driven by the tuberal

region, particularly the superior tuberal region. The novel methodology presented here will be critical for better understanding hypothalamic structural and functional abnormalities in psychiatric disorders and can aid the development of treatment if incorporated into sex-specific approaches to gene and drug discovery involving the hypothalamus.

References

Augustinack, J.C., van der Kouwe, A.J.W., Blackwell, M.L., Salat, D.H., Wiggins, C.J., Frosch, M.P., Wiggins, G.C., Potthast, A., Wald, L.L., Fischl, B.R., 2005. Detection of entorhinal layer II using Tesla magnetic resonance imaging. Ann. Neurol. 57, 489–494.

Bao, A.M., Swaab, D.F., 2007. Gender difference in age-related number of corticotropin-releasing hormone-expressing neurons in the human hypothalamic paraventricular nucleus and the role of sex hormones. Neuroendocrinology 85, 27–36.

Bao, A.M., Swaab, D.F., 2011. Sexual differentiation of the human brain: relation to gender identity, sexual orientation and neuropsychiatric disorders. Front. Neuroendocrinol. 32, 214–226.

Bao, A.M., Hestiantoro, A., Van Someren, E.J., Swaab, D.F., Zhou, J.N., 2005. Colocalization of corticotropin-releasing hormone and oestrogen receptor-alpha in the paraventricular nucleus of the hypothalamus in mood disorders. Brain 128, 1301–1313.

Baroncini, M., Jissendi, P., Catteau-Jonard, S., Dewailly, D., Pruvo, J.P., Francke, J.P., Prevot, V., 2010. Sex steroid hormones-related structural plasticity in the human hypothalamus. Neuroimage 50, 428–433.

Baroncini, M., Jissendi, P., Balland, E., Besson, P., Pruvo, J.P., Francke, J.P., Dewailly, D., Blond, S., Prevot, V., 2012. MRI atlas of the human hypothalamus. Neuroimage 59, 168–180.

Bouix, S., Martin-Fernandez, M., Ungar, L., Nakamura, M., Koo, M.S., McCarley, R.W., Shenton, M.E., 2007. On evaluating brain tissue classifiers without a ground truth. Neuroimage 36, 1207–12024.

Braitenberg, V., Schuz, A., 1998. Statistics and geometry of neuronal connectivity. Cortex. Springer, Heidelberg, p. 249.

Caviness Jr., V.S., Lange, N.T., Makris, N., Herbert, M.R., Kennedy, D.N., 1999. MRI-based brain volumetrics: emergence of a developmental brain science. Brain Dev. 21, 289–295.

Cho, Z.-H., Kim, Y.-B., Han, J.-Y., Min, H.-K., Kim, K.-N., Choi, S.-H., Veklerov, E., Shepp, L.A., 2008. New brain atlas—mapping the human brain in vivo with 7.0 T MRI and comparison with postmortem histology: will these images change modern medicine? Int. J. Imaging Syst. Technol. 18, 2–8.

Déjerine, J.J., 1895. Anatomie des centres nerveux. Rueff, Paris.

Drenhaus, U., Schingnitz, G., Dorka, M., 1986. A method for a quantitative determination of changes in tissue volume as a result of perfusion fixation. Anat. Anz. 161, 327–332.

Duvernoy, H., 1999. Surface, Three-Dimensional Sectional Anatomy with MRI, and Blood Supply. The Human Brain. Springer, Wien, NY.

Filipek, P.A., Richelme, C., Kennedy, D.N., Caviness Jr., V.S., 1994. The young adult human brain: an MRI-based morphometric analysis. Cereb. Cortex 4, 344–360.

Fischl, B., Rajendran, N., Busa, E., Augustinack, J., Hinds, O., Yeo, B.T.T., Mohlberg, H., Amunts, K., Zilles, K., 2008. Cortical folding patterns and predicting cytoarchitecture. Cereb. Cortex 18, 1973–1980.

Goldstein, J.M., 2006. Sex, hormones and affective arousal circuitry dysfunction in schizophrenia. Horm. Behav. 50, 612–622.

Goldstein, J.M., Seidman, L.J., Horton, N.J., Makris, N., Kennedy, D.N., Caviness Jr., V.S., Faraone, S.V., Tsuang, M.T., 2001. Normal sexual dimorphism of the adult human brain assessed by in vivo magnetic resonance imaging. Cereb. Cortex 11, 490–497.

Goldstein, J.M., Jerram, M., Poldrack, R., Ahern, T., Kennedy, D.N., Seidman, L.J., Makris, N., 2005. Hormonal cycle modulates arousal circuitry in women using functional magnetic resonance imaging. J. Neurosci. 25, 9309–9316.

Goldstein, J.M., Seidman, L.J., Makris, N., Ahern, T., O'Brien, L.M., Caviness, V.S., Kennedy, D.N., Faraone, S.V., Tsuang, M.T., 2007. Hypothalamic abnormalities in schizophrenia: sex effects and genetic vulnerability. Biol. Psychiatry 61, 935–945.

Goldstein, J.M., Jerram, M., Abbs, B., Whitfield-Gabrieli, S., Makris, N., 2010. Sex differences in stress response circuitry activation dependent on female hormonal cycle. J. Neurosci. 30, 431–438.

Goldstein, J.M., Holsen, L.M., Handa, R., Tobet, S., 2012. Sex differences in HPA and HPG axes dysregulation in major depressive disorder: the role of shared brain circuitry between hormones and mood. In: Pfaff, D., Christen, Y. (Eds.), Research Perspectives in Endocrine Interactions: Multiple Origins of Sex Differences in Brain: Neuroendocrine Functions and Their Pathologies. Springer-Verlag, Berlin.

Handa, R., Burgess, L., Kerr, J., O'Keefe, J., 1994. Gonadal steroid hormone receptors and sex differences in the hypothalamo-pituitary-adrenal axis. Horm. Behav. 28, 464–476.

Herman, J.P., Ostrander, M.M., Mueller, N.K., Figueiredo, H., 2005. Limbic system mechanisms of stress regulation: hypothalamo-pituitary-adrenocortical axis. Prog. Neuropsychopharmacol. Biol. Psychiatry 29, 1201–1213.

Holsen, L.M., Spaeth, S.B., Lee, J.H., Ogden, L.A., Klibanski, A., Whitfield-Gabrieli, S., Goldstein, J.M., 2011. Stress response circuitry hypoactivation related to hormonal dysfunction in women with major depression. J. Affect. Disord. 131, 379–387.

Holsen, L.M., Lee, J.H., Spaeth, S.B., Ogden, L.A., Klibanski, A., Whitfield-Gabrieli, S., Sloan, R.P., Goldstein, J.M., 2012. Brain hypoactivation, autonomic nervous system dysregulation, and gonadal hormones in depression: a preliminary study. Neurosci. Lett. 514, 57–61.

Jovicich, J., Czanner, S., Han, X., Salat, D., van der Kouwe, A., Quinn, B., Pacheco, J., Albert, M., Killiany, R., Blacker, D., Maguire, P., Rosas, D.H., Makris, N., Gollub, R., Dale, A.M., Dickerson, B., Fischl, B., Maguire, P., 2009. MRI-derived measurements of human subcortical, ventricular and intracranial brain volumes: reliability effects of scan sessions, acquisition sequences, data analyses, scanner upgrade, scanner vendors and field strengths. Neuroimage 46, 177–192.

Koh, E., Ricardo, J., 1978. Anatomical evidence of direct projections from the nucleus of the solitary tract to the hypothalamus, amygdala, and other forebrain structures in the rat. Brain Res. 153, 1–26.

Lemaire, J.J., et al., 2011. White matter connectivity of human hypothalamus. Brain Res. 1371, 46–64.

Mai, J.K., Assheuer, J., Paxinos, G., 1997. Atlas of the human brain, 1st ed. Academic Press, San Diego.

Majdic, G., Tobet, S., 2011. Cooperation of sex chromosomal genes and endocrine influences for hypothalamic sexual differentiation. Front. Neuroendocrinol. 32, 137–145.

Makris, N., 1999. Delineation of Human Association Fiber Pathways Using Histologic and Magnetic Resonance Methodologies [dissertation]. Boston University School of Medicine, Boston, MA, p. 176.

Makris, N., Schlerf, J.E., Hodge, S.M., Haselgrove, C., Albaugh, M.D., Seidman, L.J., Rauch, S.L., Harris, G.W., Biederman, J., Caviness, V.S., Kennedy, D.N., Schmahmann, J.D., 2005. MRI-based surface-assisted parcellation of human cerebellar cortex: an anatomically specified method with estimate of reliability. Neuroimage 25, 1146–1160.

Makris, N., Kaiser, J., Haselgrove, C., Seidman, L.J., Biederman, J., Boriel, D., Valera, E.M., Papadimitriou, G.M., Fischl, B., Caviness, V.S., Kennedy, D.N., 2006. Human cerebral cortex: a system for the integration of volume- and surface-based representations. Neuroimage 33, 139–153.

McClellan, K.M., Stratton, M.S., Tobet, S.A., 2010. Roles for gamma-aminobutyric acid in the development of the paraventricular nucleus of the hypothalamus. J. Comp. Neurol. 518, 2710–2728.

Mouritzen Dam, A., 1979. Shrinkage of the brain during histological procedures with fixation in formaldehyde solutions of different concentrations. J. Hirnforsch. 20, 115–119.

Nieuwenhuys, R., Voogd, J., van Huijzen, C., 2008. The Human Central Nervous System, 4th ed. Springer.

Nolte, J., 2009. The Human Brain: An Introduction to its Functional Anatomy, 6th edition. Mosby Elsevier, Philadelphia.

O'Kusky, J., Colonnier, M., 1982. A laminar analysis of the number of neurons, glia, and synapses in the adult cortex (area 17) of adult macaque monkeys. J. Comp. Neurol. 210, 278–290.

Parent, A., 1996. Carpenter's Human Neuroanatomy. Williams and Wilkins, Media, PA.

Raznahan, A., Lee, Y., Stidd, R., Long, R., Greenstein, D., Clasen, L., Addington, A., Gogtay, N., Rapoport, J.L., Giedd, J.N., 2010. Longitudinally mapping the influence of sex and androgen signaling on the dynamics of human cortical maturation in adolescence. Proc. Natl. Acad. Sci. U. S. A. 107, 16988–16993.

Romeis, B., 1968. Mikroskopische Technik. Oldenbourg Verlag, Munchen.

Saper, C.B., Chou, T.C., Elmquist, J.K., 2002. The need to feed: homeostatic and hedonic control of eating. Neuron 36, 199–211.

Schuz, A., Palm, G., 1989. Density of neurons and synapses in the cerebral cortex of the mouse. J. Comp. Neurol. 286, 442–455.

Stephan, H., 1960. Methodische Studien Uber den quantitativen Vergleich architektonischer Struktureinheiten des menschlichen Gehirns. Z. Wiss. Zool. 164, 1–2.

Stratton, M.S., Searcy, B.T., Tobet, S.A., 2011. GABA regulates corticotropin releasing hormone levels in the paraventricular nucleus of the hypothalamus in newborn mice. Physiol. Behav. 104, 327–333.

Swaab, D.F., 2003. The Human Hypothalamus: Basic and Clinical Aspects. Part I: Nuclei of the Human Hypothalamus. Handb. Clin. Neurol. 79, 476.

Swaab, D.F., 2004. The Human Hypothalamus: Basic and Clinical Aspects. Part II: Neuropathology of the Human Hypothalamus and Adjacent Brain Structures. Handb. Clin. Neurol. 80, 597.

Swanson, L.W., 2000. Cerebral hemisphere regulation of motivated behavior. Brain Res. 886, 113–164.

Swanson, L.W., Sawchenko, P.E., 1983. Hypothalamic integration: organization of the paraventricular and supraoptic nuclei. Annu. Rev. Neurosci. 6, 269–324.

Tobet, S.A., Fox, T.O., 1992. Sex Differences in Neural Morphology Influenced Throughout Life. In: Gerall, A., Moltz, H., Ward, I.L. (Eds.), Sexual Differentiation: A Lifespan Approach. Plenum Press, New York, pp. 41–83.

Tobet, S., Knoll, J.G., Hartshorn, C., Aurand, E., Stratton, M., Kumar, P., Searcy, B., McClellan, K., 2009. Brain sex differences and hormone influences: a moving experience? J. Neuroendocrinol. 21, 387–392.

Werner, L., Winkelman, E., 1976. Studies on the structure of thalamo-cortical projection neurons and interneurons in the Corpus geniculatum laterale pars dorsalis of albino rats after different histological treatments. Anat. Anz. 139, 142–157.

Zuloaga, D.G., Carbone, D.L., Hiroi, R., Chong, D.L., Handa, R.J., 2011. Dexamethasone induces apoptosis in the developing rat amygdala in an age-, region-, and sex-specific manner. Neuroscience 199, 535–547.